A deeper study on propionic acid-related inhibition during anaerobic digestion: insights on methane production and identification of biomarker candidates for an early warning

Xiaojun Liu[1], Chloé Soulard[1, 2], Véronique Jamilloux[3], André Pauss[1], Laura André[4], Thierry Ribeiro[1], Sabrina Guérin-Rechdaoui[5], Vincent Rocher[5], Carlyne Lacroix[5], Chrystelle Bureau[3], Cédric Midoux[3-5-6], Olivier Chapleur[3], Ariane Bize[3], Céline Roose-Amsaleg[2]

1 Université de technologie de Compiègne, ESCOM, TIMR, Alliance Sorbonne Université, Compiègne, France

2 CNRS UMR 6553 Ecobio, Université Rennes 1, 35000, Rennes France

3 Université Paris-Saclay, INRAE, PROSE, 92761, Antony, France

4 Institut Polytechnique UniLaSalle, Université d'Artois, ULR 7519, Rue Pierre Waguet, BP 30313, CEDEX, 60026 Beauvais, France

5 SIAAP, Innovation department, 82 avenue Kléber, 92700 Colombes, France

6 Université Paris-Saclay, INRAE, MaIAGE, 78350, Jouy-en-Josas, France

7 Université Paris-Saclay, INRAE, BioinfOmics, MIGALE bioinformatics facility, 78350, Jouy-en-Josas, France

Corresponding author: ariane.bize@inrae.fr

Keywords: propionic acid; propionate; NaCl; pH; 16S rDNA metabarcoding; municipal sewage sludge;

Abstract

Inhibition by propionic acid is a major challenge for the smooth operation of anaerobic digestion (AD) of sewage sludge for biogas production. We conducted an original study to better understand the respective roles of propionic acid, its conjugate base propionate and pH in the AD inhibition, and to identify potential inhibition biomarkers for an early warning. We focused on both methane production and microbial community composition, during the digestion of wastewater treatment sludge. A partial decrease in methane production was detected with the addition of 13 mM of propionic acid (1,000 $mg.L^{-1}$), while total inhibition occurred for 81 mM (6,000 $mg.L^{-1}$). Comparisons with the effects of adding sodium propionate, sodium chloride, and lowering the pH indicated that this inhibition was largely attributed to the H^+ counter-ion. In particular, only moderate inhibition was observed when adding sodium propionate at a concentration of 81 mM. The composition of the microbial communities was significantly modified in the presence of propionate, with this adaptation specifically depending on the nature and concentration of the compound added, more precisely of the counterion. Various functional groups were affected, including syntrophs and methanogenic archaea. The relative abundance of the latter decreased significantly in the presence of propionic acid, consistent with the negative effects observed on the methane production rate, and with previous studies. Several microbial groups highly sensitive to propionic acid were identified in both our tests, in particular the family ST-12K33 (order Sphingobacteriales), which emerged as a strong biomarker candidate.

1. Introduction

Anaerobic digestion (AD) is an environmental biotechnology process that produces renewable energy (biogas) from organic waste. For the last two decades, AD has been widely practiced and encouraged by authorities worldwide. In 2009, the European Directive 2009/28/EC aimed to increase the share of renewable energy in EU's total energy mix to 20%. One of the major waste resources feeding anaerobic digesters is municipal sewage sludge (MSS) (Scarlat et al., 2018) defined as solid/liquid residues originating from different processes in wastewater treatment plants (WWTPs). It is rich in purifying biomass and organic matter separated from wastewater. In 2017, 1.2 million tons (Mt) of dry matter (DM) MSS were produced in France, requiring effective valorization methods (EUROSTAT).

During AD, four principal interrelated biochemical processes mediated by microbes occur successively: hydrolysis, acidogenesis, acetogenesis and methanogenesis (Shrestha et al., 2020). During acidogenesis, long-chain fatty acids, amino acids as well as carbohydrates are converted into volatile fatty acids (VFAs), including acetic acid, propionic acid, butyric acid, iso-butyric acid, and others. These VFAs may subsequently be consumed by acetogenic microorganisms producing acetic acid, H_2 and CO_2, which are the main precursors for methane synthesis. However, VFAs are also major inhibitors of AD, potentially leading to AD failure (Chen et al., 2008), as they can accumulate due to an imbalance between acid production and consumption mediated by acidogenic and acetogenic bacteria (reviewed in (Alavi-Borazjani et al., 2020).

Propionic acid content (HPr) is considered as an indicator predicting the dysfunction of AD since HPr can accumulate in case of process dysfunction and is also toxic to the microbial activities. Many possible inhibition mechanisms related to HPr have been reported. HPr, along with other VFAs, is responsible for the acidification of digesters by decreasing the pH (Sawyer et al., 1954). Undissociated propionic acid, a form favored by lower extracellular pH (acidified condition), penetrates the intracellular medium and dissociates there. The dissociation causes a decrease in intracellular pH. To remediate this and maintain the proton gradient necessary for ATP formation,

the cell actively transports protons to the extracellular medium, thereby reducing the ATP available for its growth and metabolism (Jiang et al., 2018). The intracellular accumulation of dissociated HPr is also toxic to microorganisms, as it increases intercellular ionic strength, which can be fatal to microbial activities (Roe Andrew et al., 1998).

The inhibition of AD related to HPr has been widely studied for a variety of organic waste. Nevertheless, the conclusions are very variable according to the study. (Pullammanappallil et al., 2001; Qiao et al., 2013; Yang et al., 2015) observed no inhibition with HPr concentration up to 50 mM (equivalent to 3700 $mg.L^{-1}$) during AD of diverse waste under both thermophilic and mesophilic conditions. In contrast (Demirel & Yenigün, 2002; Wang et al., 2009) reported a decrease in biogas yield at HPr concentrations below 12.2 mM (903 $mg.L^{-1}$). (Han et al., 2020) concluded that reversible inhibition with an increased lag phase could occur at HPr concentrations above 22.7 mM (1680 $mg.L^{-1}$). This variability is likely due to differences in the nature of the substrate and inoculum, as well as other operating conditions. In particular, propionic acid (Demirel & Yenigün, 2002; Wang et al., 2009) or sodium propionate (NaPr) (Yang et al., 2015) were used, with obvious different effects. This highlights the need for further research to better disentangle the effects of these different parameters through comparative analysis.

The composition of microbial communities from anaerobic digesters is also of interest but has been poorly investigated during propionic acid inhibition. AD microbial communities in general are diverse (Calusinska et al., 2018; Campanaro et al., 2016; Sikora et al., 2017) and characterized by various and numerous ecological interactions, such as competition or syntrophy (Sikora et al., 2017; Westerholm et al., 2022). Syntrophy, in particular, is essential for maintaining the low H_2 partial pressure required for acetogenesis (Sikora et al., 2017; Westerholm et al., 2022). The composition of the microbial communities is specific to each digester (Theuerl et al., 2018). However, when considering a given type of feeding, several studies suggest the existence of a core microbiota, present in the vast majority of digesters and responsible for most of the catalytic activity (Calusinska et al., 2018; Kirkegaard et al., 2017), in agreement with Pareto principle

(Verstraete & Mertens, 2004). This opens up the possibility of establishing microbial process management by identifying robust biomarkers (Krohn et al., 2022). During anaerobic digestion, propionate is converted by propionate oxidizers, particularly syntrophic propionate oxidizing bacteria (SPOB) interacting with acetogenic and hydrogenotrophic methanogens (reviewed in (Westerholm et al., 2022)). These two functional groups are therefore likely to be affected by the presence of propionate and are also known to be more sensitive to perturbations compared to hydrolytic and acidogenic bacteria (Sikora et al., 2017). According to previous studies, a shift from acetoclastic to hydrogenotrophic methanogenesis enabled the recovery of a digester inhibited by HPr (Han et al., 2020). By contrast, (Li et al., 2017) suggested the positive role of *Methanosaetaceae*, which comprises exclusively acetoclastic methanogens, during propionate degradation in the presence of high ammonia concentrations. This further emphasizes the specificity of the microbial response to given operating parameters.

In the present study, we specifically focused on municipal wastewater sludge digestion and we tackled the following questions: How does the presence of HPr affect the physico-chemical dynamics of AD as a function of its concentration? Is the observed inhibition primarily due to the presence of dissociated propionate or to the drop in pH caused by HPr dissociation? Finally, to what extent do microbial communities adapt to the presence of HPr, and can any relevant candidate biomarkers of early inhibition be identified?

To address these issues, we conducted two series of tests in mesophilic AD batch microcosms. In the first tests, we focused on the effects of HPr concentration on both physico-chemical parameters and microbial community composition in a longitudinal study. In the second tests, we played on the pH, the nature of the propionate counterion, or other added compounds, to discern the respective contributions of pH and dissociated propionate to the observed inhibition. In this second tests, microbial community composition was analyzed especially at the final time points.

2. Material and methods

2.1 Experimental study on propionic acid inhibition

2.1.1 Origin of inocula and substrates

Propionic acid inhibition experiments were conducted in AD reactors using a mixture of substrate and inoculum. The substrate was a mixture of primary, biological, and tertiary MSS collected from the Seine-Aval wastewater treatment plant (WWTP), which processes 1 500 000 m^3 per day and serves the Paris conurbation (France). The digested sludge used as inoculum was obtained from one of the mesophilic digesters at the same Seine-Aval WWTP. Different batches of both types of sludge were utilized for each test series, consistently sourced from the same sampling points. The total solid content (TS), volatile solid content (VS), and pH of the substrate ranged from 3.3% to 4.7% of fresh mass, 71% to 77% of TS and 6.0 to 6.3, respectively. For the inoculum, these values were 2.3% to 2.6%, 61% to 63% of TS, and 7.4 to 7.6, respectively (Table S1).

2.1.2 Anaerobic digestion tests

Two series of Biochemical Methane Potential (BMP) tests were conducted and involved different treatments. Except for the controls (Neg, Ctrl), the treatments were named according to the compound specifically added to the reactors and its molar concentration, if relevant (e.g.: treatment HPr20 when 20 mM HPr were added, HCl when HCl was added, etc, Table S2).

In more details, the first tests (Table S2) aimed to investigate the effect of HPr on AD dynamics, particularly to determine the inhibitory threshold for the utilized substrate-inoculum pair. The incubations were conducted using the AMPTS II (II (Automatic Methane Potential Test System II, Bioprocess, Lund, Sweden), in batch and mesophilic (37°C) conditions. Biochemical Methane Potential (BMP) tests were prepared by following the guidelines of (Holliger et al., 2016). Each 500 mL reactor was filled with 100 mL of inoculum (fresh MSS), 100 mL of substrate (digested MSS), and 200 mL of deionized water to reach a working volume of 400 mL. Additionally, either 0, 13, 20, or 81 mM of HPr was initially added, corresponding to four distinct treatments: Ctrl,

HPr13, HPr20 and HPr81. In total, 30 AD reactors were operated: 8 for each treatment, except that only 6 reactors under HPr13 were set up. To analyze microbial communities during the course of AD, two reactors from each treatment were sacrificed on days 2, 4, 7, and 13, to collect their content, except for treatment HPr13 that was not analyzed on day 13.

The second tests (Table S1) were conducted to identify the direct cause of AD process inhibition when HPr is added. The conditions were similar to those of the first test: the operation was conducted for 22 days under mesophilic conditions (37°C) using AMPTS II, with a working volume of 400 mL. Eight distinct treatments were established, each in triplicates unless otherwise stated. The controls without substrate (Neg, 6 replicates) contained the inoculum (200 mL) and deionized water (200 mL). The controls without disturbance (Ctrl, 5 replicates) were filled with both inoculum (200 mL) and substrate, i.e. MSS (200 mL). For the remaining six treatments, inoculum (200 mL) and MSS (200 mL) were added along with one of the following: 20 mM HPr (HPr20), 81 mM HPr (HPr81), 20 mM NaPr (NaPr20), 81 mM NaPr (NaPr81), 81 mM NaCl (NaCl81); or a dropwise addition of a 10% HCl solution to obtain an initial pH of 5.1, the same as under HPr81. This represented 29 reactors. The liquid phase was sampled for chemical and microbial analysis exclusively prior incubation and at the final time point. Homogenized samples were kept frozen until subsequent molecular analysis.

2.1.3 Curve modeling by modified Gompertz equation

AMPTS recorded daily methane production for each reactor. The data were processed using Office Excel 2019 (Microsoft®, Redmond, US). The modified Gompertz equation (**Equation 1**) was used to estimate the kinetic parameters related to methane production for each treatment. Non-linear regression for kinetic modeling was performed using Scilab software (Dassault Systèmes, Vélizy-Villacoublay, France). The model's goodness-of-fit was evaluated based on adjusted R^2, sum of squared errors (SSE), root mean squared errors (RMSE) and mean absolute percentage error (MAPE).

$$BMP(t) = BMP_0 / \{ 1 + \exp [R_m \cdot e \cdot (\lambda - t) / BMP_0 + 1]\}$$ (**Equation 1**)

where BMP(t) is the cumulative methane production at time t ($NL_{CH4} \cdot kg_{VS}^{-1}$), BMP_0 is the maximum methane yield of the substrate tested ($NL_{CH4} \cdot kg_{VS}^{-1}$), R_m is the maximum methane yield rate ($NL_{CH4} \cdot kg_{VS}^{-1} . d^{-1}$), λ is the lag time (d), t is the incubation duration (d) and e ≈ 2.7182.

ANOVA followed by a post hoc Tukey test were performed using R Studio (R Studio Inc., Massachusetts, USA) to assess significant differences between experimental results.

2.2 Microbial community analysis

2.2.1 DNA extraction

For all sample types (inoculum, substrate, reactor content), DNA extraction was conducted in a randomized order using the kit Nucleobond® RNA Soil (Macherey-Nagel, Düren, Germany) following the manufacturer's instructions. The DNA Set was included because it is designed for samples with a complex matrix. Mechanical cell lysis was performed with TissueLyser II (Qiagen, Hilden, Germany) during the initial step. The final elution was carried out with 100 µL of RNase-free water. DNA concentrations were measured using Quantifluo with a SAFAS spectrophotometer, employing the fluorescent dye Picogreen® (ThermoFisher, Waltham, US).

2.2.2 16S rRNA gene amplicon sequencing

Sequencing of 16S rDNA amplicons was performed using an Ion torrent PGM instrument (Life Technologies, Carlsbad, US) after PCR amplification of the V4-V5 hypervariable regions with the following fusion primers: 515F (5'-Ion A adapter - Barcode – GTGYCAGCMGCCGCGGTA- 3') and 928R (5'- Ion trP1 adapter – ACTYAAAKGAATTGRCGGGG-3') (Table S3). The detailed protocol for this procedure has been previously described (Poirier et al., 2016).

A total of 36 samples were processed for the first tests, and 29 samples for the second tests (Table S2). The raw reads were submitted to the ENA under project accession PRJEB87704.

2.2.3 Bioinformatic processing

The raw amplicon sequencing data were pre-processed with deepomics16S pipeline (https://forgemia.inra.fr/cedric.midoux/deepomics16S v 14.10.2022) on the servers of the INRAE MIGALE bioinformatics platform. This pipeline primarily employs DADA2 (Callahan et al., 2016), for the generation of Amplicon Sequencing Variants (ASVs) and FROGS (Bernard et al., 2021) for the taxonomic affiliation of ASVs through alignment with blast against the Silva database, version silva_138.1_16S_pintail100. Due to a lower sequence quality obtained for the second tests, only the V4 region was considered for theses samples, using primer sequences 5'-GTGYCAGCMGCCGCGGTA and 5'-GGACTACHVGGGTWTCTAAT for trimming.

The sequencing depth was sufficient, with each sample retaining more than 15,000 sequences after bioinformatics processing (Figure S1). The raw sequences, biom files and physicochemical data were deposited in the DeepOmics information system (https://deepomics.inrae.fr/home).

2.2.4 Biostatistics analysis

The pre-processed sequencing data were analyzed using R version 4.3.2 (Team, 2021) in RStudio (2024.04.2+ 764) environment. Several specific packages were utilized, such as ComDim 0.9.51 (https://github.com/f-puig/R.ComDim) for Common Component Analysis (CCA), mixOmics 6.26.0 (Rohart et al., 2017) for principal component analysis (PCA), DESeq2 1.42.0 (Love et al., 2014) for differential abundance analysis and phyloseq 1.46.0 (McMurdie & Holmes, 2013) for other analyses or representation. The taxonomic tree was built with GraPhlAn (https://github.com/biobakery/graphlan).

For data from the first tests, 157 Amplicon Sequence Variants (ASVs) were selected, by removing the ASVs with fewer than 400 reads in the dataset. For the second tests, ASVs representing less than 0.5% of the reads in the dataset were removed, resulting in 169 ASVs for analysis, a number similar to the first tests. However, for the differential analysis, data from the second tests were

filtered less strictly, removing ASVs representing less than 400 reads, resulting in a total of 276 ASVs.

3. Results

3.1 Inhibition of methane production increases with propionic acid concentration

To study AD inhibition by HPr, we focused on four distinct concentrations of added HPr: 0, 13, 20 and 81 mM (first tests of this study), aiming to obtain contrasted inhibition levels (Table S2). Based on cumulative methane production, a gradual increase in inhibition occurred as the concentration of added HPr increased, with complete inhibition occurring under HPr81 (Figure 1A). Additionally, the pH values overall decreased with increasing HPr concentration (Figure S2), which can be explained by both the dissociation of the added HPr and the accumulation of other volatile fatty acids due to acidic inhibition of the process. Indeed, under HPr81, the pH values remained at 5 or 5.1 throughout the entire incubation period. Such pH values are known to inhibit the AD process, especially methanogenesis (Clark & Speece, 1971).

3.2 Methane production is more sensitive to acidic pH and HPr than to propionate ion

The negative effect on methane production following HPr addition may be attributed to the propionic acid itself, its ionized form (propionate, Pro^{-}) and/or the low pH condition caused by HPr dissociation, generating protons (H^{+}). To investigate different possible effects, six distinct incubation conditions were established in addition to the controls in second AD tests, by varying the nature of the counterions or targeting specific pH values (Materials and methods, Table S2). Because the same molar concentration was used for different treatments (e.g. 20 mM HPr or 20 mM NaPr, etc) pairwise comparisons between the treatments enabled the investigation of the specific effects of certain ions. Comparison of HPr20 and NaPr20 on the one hand, HPr81 and NaPr81 on the other, enabled to assess the contribution of acidity to the observed effects (H+ compared to Na+). In addition, NaCl81 treatment aimed to verify the absence of inhibition by

sodium ions (Na^+) (Chen et al., 2008). Finally, HCl was added to obtain an initial pH value of 5.1, the same as that measured under HPr81. This last condition enabled the comparison with a pH decrease of similar magnitude that was not caused by the addition of HPr. Besides, treatments HPr20 and HPr81 also enabled comparison with the first tests.

After 22 days of incubation, the cumulative methane production of MSS under the different conditions was calculated by subtracting the mean gas production of the negative controls from the respective raw methane productions. The negative controls yielded 56 ± 2 $NL_{CH4}.kg_{VS}^{-1}$, which meets the acceptance criteria for BMP validity (Holliger et al., 2016). The results are presented in Figure 1B and the relevant kinetic parameter values for each condition are provided in Table 1.

It can be concluded that Ctrl yielded 250 $NL_{CH4}.kg_{VS}^{-1}$, with no significant difference compared to the production under NaCl81 (253 $NL_{CH4}.kg_{VS}^{-1}$). This indicates that the concentrations of Na^+ and Cl^- ions tested ($[Na^+] = [Cl^-] = 81$ mM) did not inhibit the AD process. By contrast, under HPr81 or HCl, both leading to an acidic pH of 5.1, no methane was ever produced.

The addition of propionate at lower levels, either in its HPr or NaPr form, contributed to a delay in methane production, as indicated by the longer lag phases (λ) compared to Ctrl (Table 1). However, it ultimately improved the methane yield (Table 1), which increased up to 348 ± 5 $NL_{CH4}.kg_{VS}^{-}1\ VS^{-1}$ for NaPr81. With the addition of HPr or Pr^-, methane was produced not only through MSS degradation, but also by the consumption of HPr or Pr-, which acted as additional substrates for the microorganisms.

The methane production under Ctrl was subtracted from that of the other treatments. and compared to the stoichiometric production of methane from propionate and propionic acid, which is 39.2 $NL_{CH4}.mol^{-1}$ according to **Equation 2**:

$$CH_3CH_2COOH + 0.5\ H_2O \rightarrow 1.75\ CH_4 + 1.25\ CO_2 \qquad (\textbf{Equation 2})$$

In Figure 1C, the comparison of NaPr and HPr treatments at the same molar concentrations highlighted the significant effect of pH and/or the undissociated form of HPr, compared to that of Pr^- ion. Methane was produced even for high propionate concentration, despite a transient

inhibition during the initial hours of the tests. The production reached almost 86% of the maximal methane production under NaPr81.

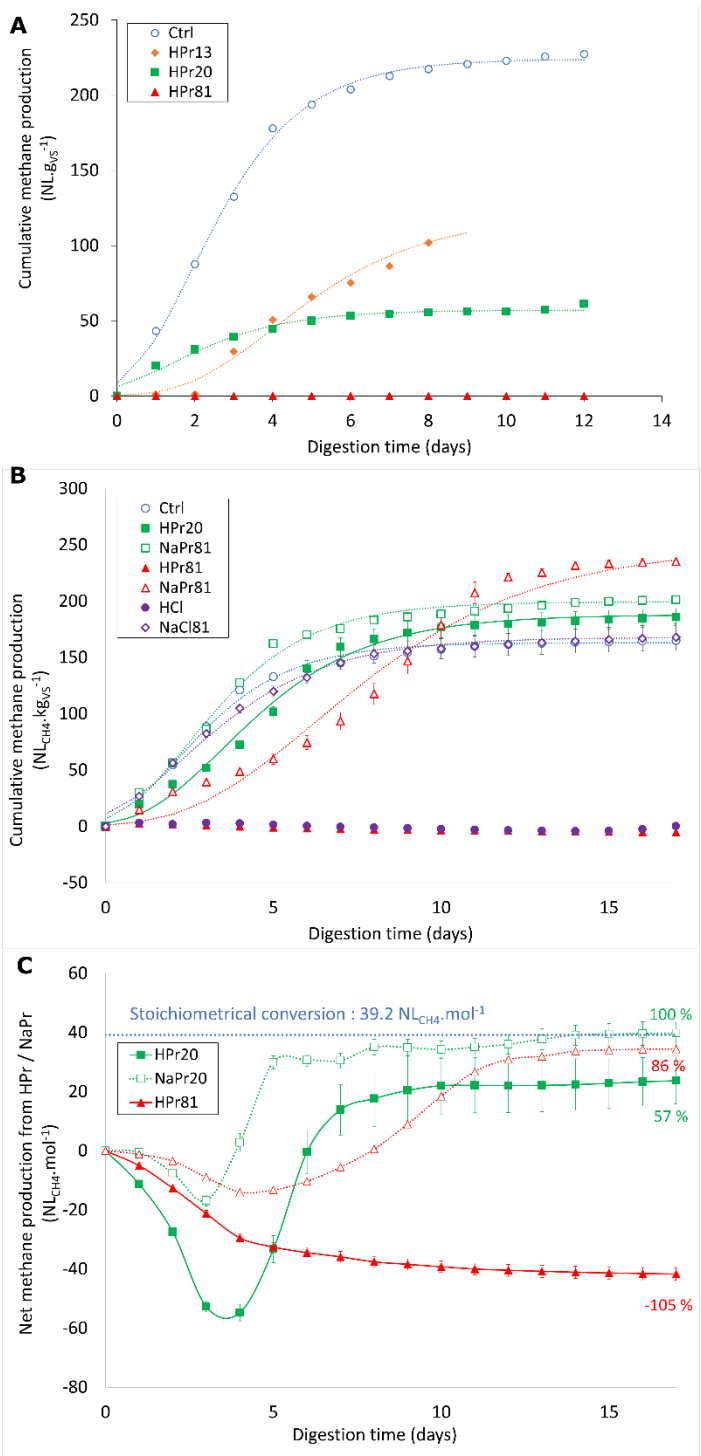

Figure 1. Methane production dynamics during AD in the first (A) and second (B, C) tests

A. Cumulative net methane production of MSS over time under the various conditions, during the first tests. **B.** Cumulative net methane production of MSS over time under the various conditions, during the second tests. **C.** Net methane production over time, obtained by subtracting methane

production in the control (Ctrl) to the methane production in the considered conditions The curves are the averages of the replicates, the dotted lines are the results of Gompertz identifications (Equation 1).

Table 1. Kinetic parameters of the modified Gompertz equation and fitting goodness for the second tests

Treatment assessed	BMP_0 (NL CH_4·kg VS^{-1})	λ (day)	R_m (NL CH_4·kg VS^{-1}·d^{-1})	MAPE* (%)	R^2 (–)
Ctrl	250 ± 2	0.35 ± 0.08	56.1 ± 3.9	2.16 ± 0.23	0.995 ± 0.002
HPr20	280 ± 14	1.13 ± 0.07	43.8 ± 2.9	8.70 ± 0.66	0.991 ± 0.001
NaPr20	291 ± 5	0.55 ± 0.01	57.8 ± 0.8	3.59 ± 0.14	0.995 ± 0.000
HPr81	NA**	NA	NA	NA	NA
NaPr81	348 ± 5	2.45 ± 0.22	33.7 ± 1.2	15.2 ± 1.0	0.981 ± 0.001
HCl	NA	NA	NA	NA	NA
NaCl81	253 ± 16	0.13 ± 0.03	43.4 ± 1.0	1.69 ± 0.14	0.996 ± 0.001

* Mean absolute percentage error of modeling
** Results are not available (NA) because the Gompertz equation was not suitable for the shape of curve
BMP0 is the maximum methane yield of the substrate tested, λ is the lag time and Rm is the maximum methane yield rate

In conclusion, the inhibition of methane production upon the addition of HPr was largely attributed to the H^+ counter-ion, which both decreased the pH and likely favored the undissociated form of propionic acid, which may be toxic to the cells. Since the effects on methane production are generally mediated by the response of the catalytic microbial communities to the operating conditions, we then focused on microbial community composition within the reactors. Our aim was to characterize its possible adaptive changes, and to identify candidate biomarkers for the early warning of HPr-induced inhibition.

3.3 Significant adaptation of microbial communities to propionic acid occurs during ecological successions

To be effective, a biomarker must meet several criteria. It must in particular demonstrate high sensitivity, in order to alert the operator to a dysfunction before significant alteration in process

performance occurs. Additionally, it must exhibit reproducibility and repeatability. In our specific case, candidate biomarkers must preferably show a marked difference in behavior between the control and treatments with moderate HPr concentrations.

To investigate the adaptive dynamics of microbial community composition in the presence of propionic acid, 16S rDNA metabarcoding was applied to 36 samples from the first tests, encompassing different treatments (Ctrl, HPr13, HPr20, HPr81), replicates, and time points. Among the 16 bacterial phyla represented, the five most abundant were Bacteroidota, Proteobacteria, Firmicutes, Chloroflexi, and Spirochaetota (Figure S3), which are commonly identified in anaerobic digesters (Calusinska et al., 2018; Jiang et al., 2021).

Archaea consistently represented less than 2% of the sequences in the different samples and were predominantly from the genera *Methanosarcina* and *Methanolinea* (Figure 2A). The first genus contains exclusively versatile methanogens whose genomes encode three distinct methanogenesis pathways (hydrogenotrophic, acetoclastic and methylotrophic) (Liu & Whitman, 2008), while the second corresponds to strictly hydrogenotrophic methanogens (Sakai et al., 2012).

The patterns of microbial community composition (Figure S4) were revealed by Principal Component Analysis (PCA), showing good reproducibility among replicates and the separation of the samples according to the treatment and the incubation time. Furthermore, based on PERMANOVA, 38% of the variance in the Bray-Curtis distance matrix was significantly explained by the HPr concentration and 24% by the time (`dist.bc ~ treatment * day of incubation`, 9999 permutations, p-value = 10^{-4} for both factors). The dynamic adaptation of microbial communities to the presence of propionic acid was thus clearly demonstrated.

Particularly noteworthy was the pronounced decrease in the proportion of reads attributed to archaea as a function of the applied propionic acid (HPr) concentration (Figure 2A). On day 13, this proportion reached nearly 3% in control reactors, between 1% and 2% in reactors with intermediate HPr concentrations, and less than 0.2% in reactors exposed to the highest HPr concentrations.

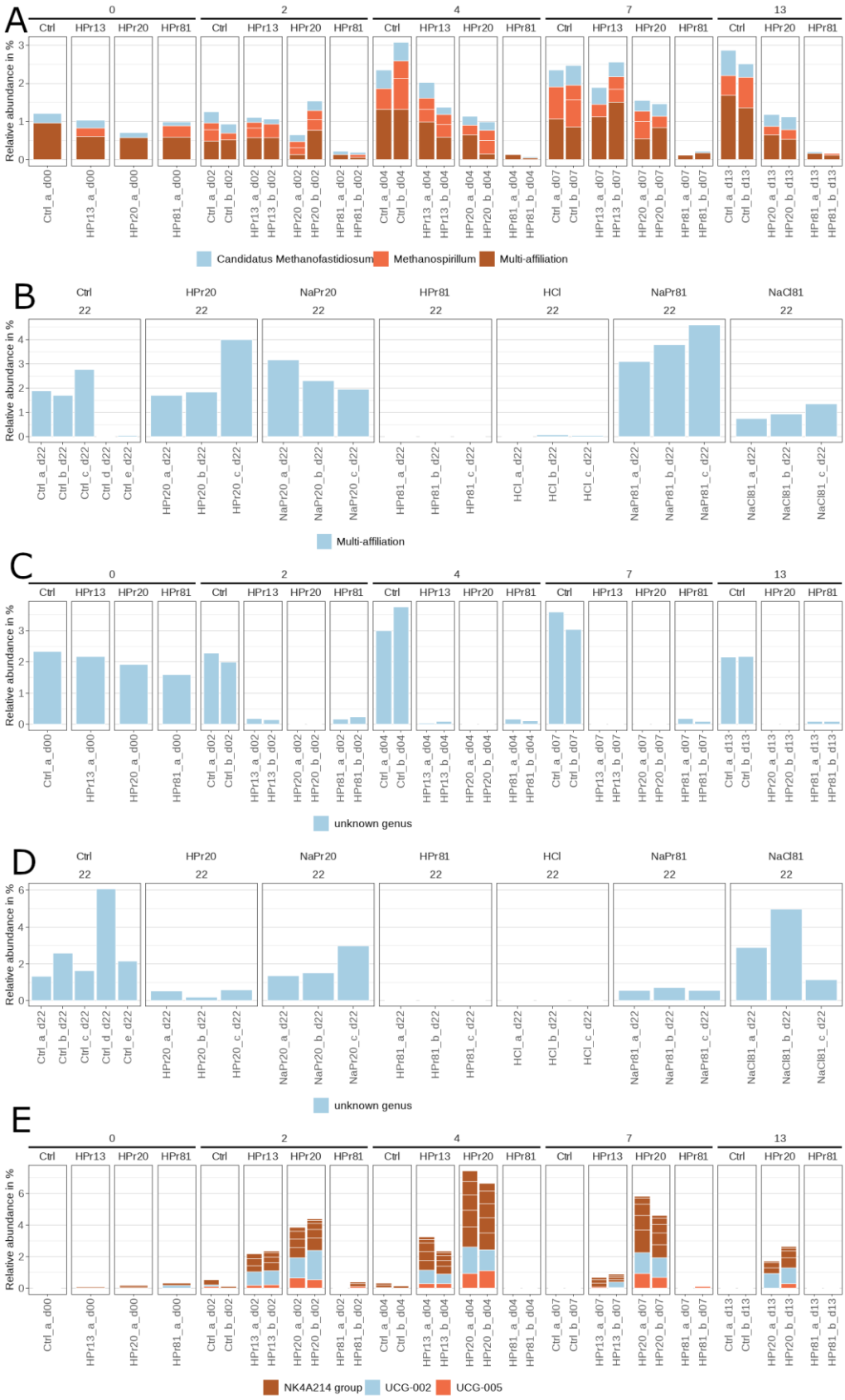

Figure 2: Barplots of selected microbial groups of interest. A. Abundance of the archaeal community in the first tests, at the genus level. B. Abundance of the archaeal community in the

second tests, at the genus level. C. Abundance of the family ST-12K33 (Sphingobacteriales order) in the first tests. D. Abundance of the family ST-12K33 (Sphingobacteriales order) in the second tests. E. Abundance of the family Oscillospiraceae in the first tests. For the first and second tests, multi-affiliation corresponds to *Methanosaeta* and/or *Methanomicrobium*, most likely *Methanosaeta.*

3.4 Common Component and Specific Weight Analysis highlights numerous microbial groups affected by HPr, as well as several early-warning biomarker candidates

To delve deeper and highlight microbial community patterns, we conducted a Common Component Analysis (CCA). With this method, "each Common Component (CC) will group together the contributions of variables that have the same effect on the dispersion of the observations", "the advantage over PCA being that the contribution of each variable to a CC is optimally weighted" (Jouan-Rimbaud Bouveresse & Rutledge, 2024). This method has been previously used for 16S metabarcoding analysis (Puig-Castellví et al., 2020). To extract relevant information from CCA, we cross-referenced different visualizations. For each CC, Figure 3A illustrates the average scores of each treatment over time: for a given CC, differential longitudinal profiles across treatments reveal distinct phenomena occurring in the various treatments. Figure 3B is a taxonomic tree representing 75 distinct ASVs underlying the longitudinal patterns observed in Figure 3A. For each CC, these ASVs were selected based on their loadings, exceeding 1.5 times the standard deviation of all ASV loadings on the respective CC (Figure S5). Finally, the temporal evolution these 75 ASVs was examined individually through relative abundance barplots (Figures S6 to S91, Table S4; a given ASV can be identified for several CCs). The relative abundance of an ASV associated to CC1 is shown in Figure 3C as an illustrative example.

Clear and distinct trends were observed across the CCs. Specifically, CC1 exhibited a particular trend for the highest HPr concentration (HPr81), noticeable from day 4 and intensifying progressively over time (Figure 3A). The 13 underlying ASVs identified for CC1 were among the

most abundant in the dataset, most of them reaching more than 5% relative abundance of reads in at least one sample. These ASVs exhibited significant diversity (Figure 3B), representing 12 distinct families and 6 distinct phyla (Figures S6 to S18, Table S4). Their longitudinal profiles were heterogeneous. Notably, four of them exhibited overall lower relative abundance under high HPr exposure (HPr81) at days 2, 4, or 7, suggesting their strong impairment at such HPr concentration. They belonged to the families Anaerolineaceae (e.g.: Figure 3C), Sedimentibacteraceae (genus *Sedimentibacter*), Dysgonomonadaceae (genus *Proteiniphilum*) and Bacteroidetes vadinHA17. Among them, ASV1 (Sedimentibacteraceae, *Sedimentibacter*) was especially worth noting regarding the early warning of AD inhibition, since it exhibited lower levels compared to the control, even with the smallest additions of HPr. In contrast, three other ASVs had higher relative abundances under the highest HPr concentration (HPr81), being likely selected by these heavy-duty conditions, and were not relevant biomarker candidates for an early warning due to their lack of sensitivity. These ASVs belonged to the families Cloacimonadaceae (genus Candidatus Cloacimonas), Tannerellaceae (genus *Macellibacteroides*), and Xanthomonadaceae (genus *Thermomonas*). The six remaining ASVs exhibited a different or more complex profile. Taken together, the ASVs associated with CC1 were predominantly various acidogens, based on MIDAS database (Dueholm et al., 2024) and on the literature. This is consistent with their high proportions, related to the abundance and diversity of fermentable molecules in the wastewater feeding sludge.

CC2 discriminated HPr81 from HPr13 and HPr20, with these differences establishing relatively rapidly between days 0 and 2 (Figure 3A). CC2 was associated to the highest number of underlying ASVs, namely 31, which belonged mostly to three phyla: Firmicutes, Bacteroidota and Proteobacteria (Figure 3B, Figures S19 to S49, Table S4) and were distributed over 22 distinct families. They likely encompassed a wide range of functional groups, such as fermenters (e.g. members of Oscillopiraceae (Gophna et al., 2017)), potential syntrophic propionate oxidizers belonging to *Smithella* (Westerholm et al., 2022) and hydrogenotrophic methanogens assigned to

Methanospirillum. They corresponded to subdominant taxa, with abundance values in samples all below 7%, and often below 1%. In good agreement with the score profiles for CC2, 12 of the 31 underlying ASVs were significantly more abundant under HPr81, and much less abundant or even undetected in the other treatments, most often from day 2 onwards. These 12 ASVs were not relevant candidate biomarkers due to their lack of sensitivity. Interestingly, 13 other ASVs showed higher relative abundances under HPr13 and/or HPr20 at one time point at least, most often from day 2 onwards (Figures S19 to S49). All of these were relevant with respect to early warning of inhibition. They belonged to eight different families, among which Oscillospiraceae stood out prominently, comprising 6 of these 13 ASVs. Two additional ASVs underlying CC2 were interesting biomarker candidates: ASV 140 (*Methanospirillum*) was negatively affected by HPr from day 7 onwards, even by the lowest additions; and ASV 17 (Sphingobacteriales, ST-12K33) was barely detected in conditions other than the control (Figure 2C).

CC3 revealed distinct evolutions between Ctrl and other treatment groups, establishing progressively between the first and the fourth days of incubation (Figure 3A) and corresponded also to subdominant ASVs. Diverse patterns emerged among the 23 underlying ASVs, each with abundances below 4% across all samples (Figures S50-S72). Of these, 13 ASVs exhibited higher abundances in the control samples from the second or fourth day of incubation. As could be anticipated, many of these 13 ASVs were relevant biomarker candidates, namely 11: they included 3 ASVs from the *Sedimentibacter* genus and 4 ASVs from *Syntrophomonas* (Figure 3B, Figures S50 to S72, Table S4). *Sedimentibacter* presumably corresponded to protein fermenters (Imachi et al., 2016). *Syntrophomonas* bacteria oxidize butyrate or saturated fatty acids, producing acetate and H_2, and, in some cases, propionate, depending on the substrate (Sekiguchi, 2015). Consequently, they can develop syntrophic interactions with hydrogenotrophic methanogens (Sousa et al., 2007). The remaining 10 underlying ASVs displayed various patterns according to the HPr concentration. Specifically, five ASVs were additional promising biomarker candidates, being on the whole less abundant in the controls than under HPr exposure, and they belonged to

five distinct families (Tannerellaceae, Butyricicoccaceae, Veillonellaceae, Comamonadaceae, Methylophilaceae).

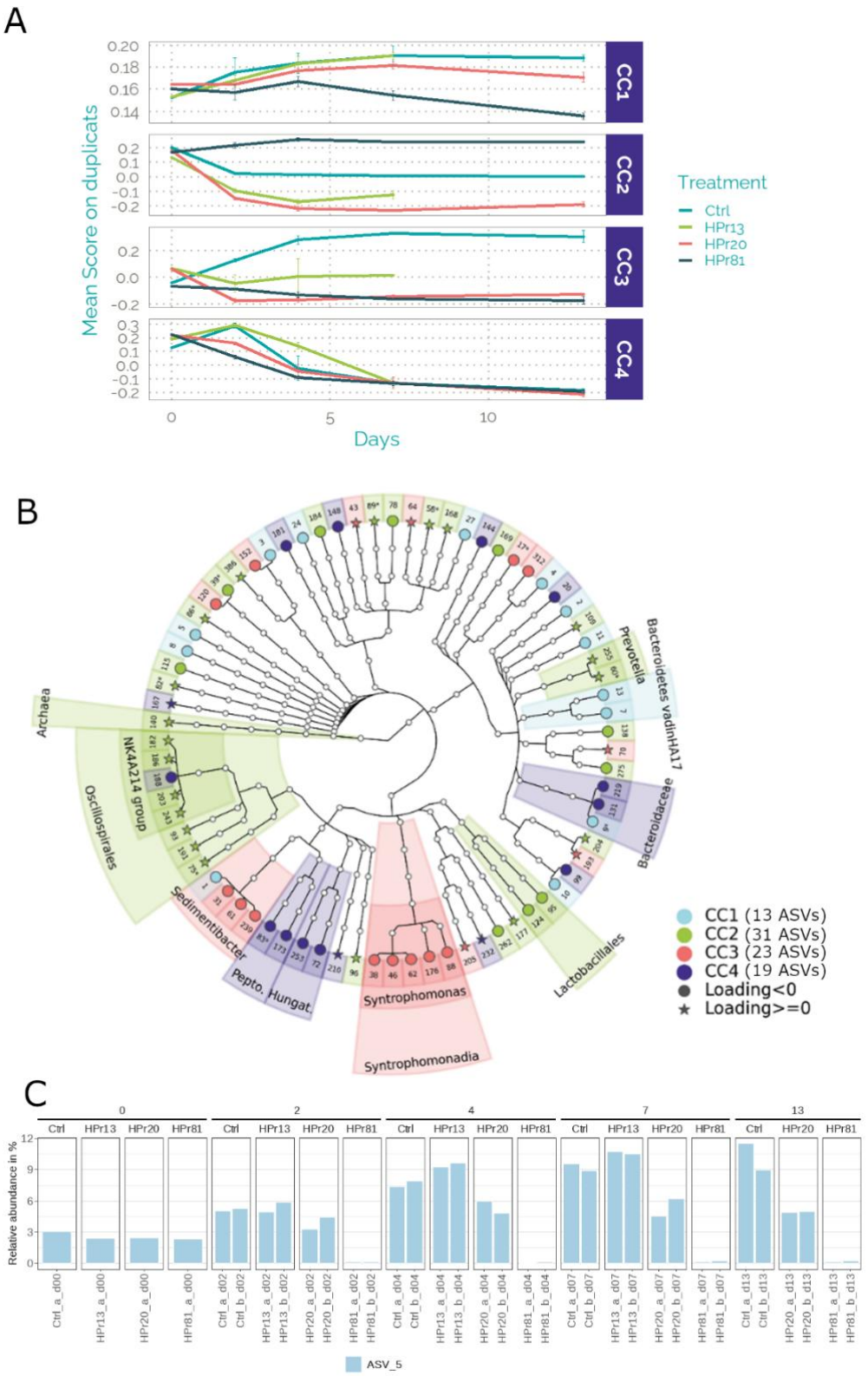

Figure 3. Illustration of the results obtained by Common Component Analysis (CCA) for the first tests. A: profiles over time (in days) of the AD reactors for the 4 first Common Components (CC); the average and standard deviation are shown, 2 replicates. B: taxonomic tree of the ASVs contributing the most to the four first CCs. C: illustrative example of an ASV associated to CC1 (ASV 5: Bacteria, Chloroflexi, Anaerolineae, Anaerolineales, Anaerolineaceae, unknown genus).

Lastly, CC4 exhibited consistent trends among the different treatments (Figure 3A), primarily reflecting temporal evolutions, with significant and rapid changes in dynamics between days 2 and 7. The 19 ASVs associated to CC4 were either dominant or sub-dominant and included 13 that decreased over time, while six exhibited an increasing trend (Figures S73 to S91, Table S4). CC4 thus reflected the ecological successions anticipated due to progressive substrate depletion and bioconversion in batch operating conditions.

Overall, CCA fully confirmed that exposure to HPr affected the abundance of numerous ASVs representing diverse functional and phylogenetic groups, which enabled us to identify a total of 35 distinct biomarker candidates for HPr inhibition (Table S4). Despite microbial adaptation, process performance was not fully maintained, as evidenced by the decrease in methane production rate, which was all the more pronounced as exposure to HPr was high. Under HPr81, methane production was actually fully inhibited; however, the changes observed in microbial community composition under this condition suggest that acidogenesis likely remained active to some extent. At this stage, several questions remained. To what extent was the adaptation of the microbial community driven by the specific compound added, and in particular, by the nature of the counterion (e.g. H^+ or Na^+)? Were the observations on microbial community repeatable?

3.5 Microbial communities overall specifically adapted to each added compound

To determine whether microbial communities adapted specifically to each compound added, we applied 16S rDNA metabarcoding to 29 samples from the second tests, collected in each reactor

at the final time point, after 22 days of incubation. Out of 18 different bacterial phyla, the dominant ones were Bacteroidota, Firmicutes, Chloroflexi, and Cloacimonadota. According to the samples, Proteobacteria, Spirochaetota, and Synergistota were also highly represented (Figure S92). This differed in part from the first tests, where Cloacimonadota was not among the most dominant phyla. Certain treatments resulted in notable differences compared to the controls, such as an increased abundance of Spirochaetota and a decreased abundance of Bacteroidota under HPr81. Additionally, Bacteroidota was more prevalent while Firmicutes was less abundant under NaCl81. The proportion of methanogenic archaea varied significantly across treatments (Figure 2B), reaching approximately 2-3% in control reactors, slightly higher proportions under NaPr conditions, and slightly lower ones under NaCl conditions, compared to Ctrl. Archaea were detected in extremely low proportions in the most inhibited reactors (HPr81 and HCl).

To identify the microbial groups specifically influenced by the treatments at a finer taxonomic level, we conducted a differential analysis, targeting the ASVs of archaea and bacteria. Several key findings emerged from this analysis. A total of 145 ASVs out of 276 were identified as differentially abundant when comparing the various treatments to Ctrl (Table S5). Among these, 122 ASVs were significantly less abundant in at least one treatment, whereas only 26 ASVs were significantly more abundant in at least one treatment (Figure 4). This suggests a negative impact of the treatments on diversity. This conclusion remains valid when considering the proportion of reads assigned to these ASVs, with the read proportion of negatively affected ASVs being higher in the controls than the read proportion of positively selected ASVs in the treated reactors (Figure 5 and Figures S93-S95).

A second key observation was the specificity of community adaptation. Each treatment, except for NaPr20, exhibited at least one ASV that was differentially abundant exclusively under that treatment (Figure 4). Besides, increasing the concentration of the compound of interest led to the detection of additional differentially abundant ASVs. For instance, 16 ASVs were detected as differentially abundant under HPr20, compared to 110 under HPr81. Similarly, 5 ASVs were

differentially abundant under NaPr20, while 27 were detected under NaPr81. This likely reflects the presence of toxicity thresholds that vary among microorganisms, with a greater number of strains being affected as the concentration increases.

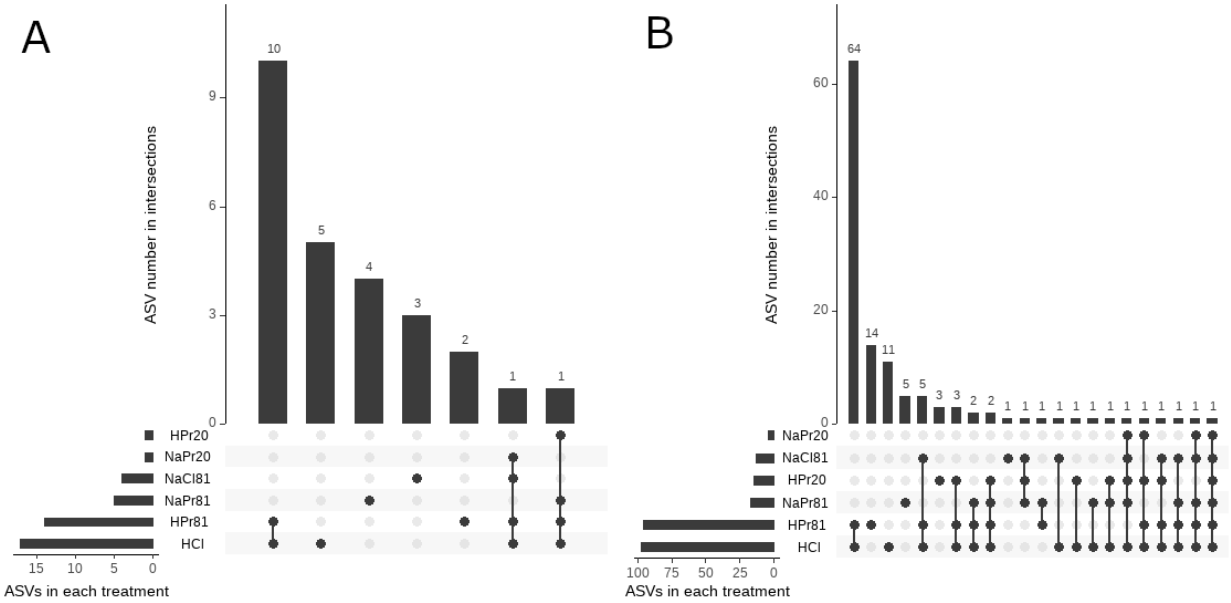

Figure 4. Upset plot of the ASVs detected as differentially abundant by comparing the different treatments to the control. (A) ASVs significantly less abundant when comparing the treatment to the control (total of 122 ASVs). (B) ASVs significantly more abundant when comparing the treatment to the control (total of 26 ASVs).

Finally, the impact of acidity on microbial communities was stronger than that of non-acidic compounds. The number of differentially abundant ASVs was consistently higher in the presence of H^+ compared to other counterions: 16 ASVs were differentially abundant under HPr20, but only 5 under NaPr20; 110 ASVs were differentially abundant under HPr81, compared to just 27 under NaPr81 and 17 under NaCl81. Supporting this conclusion, the number of differentially abundant ASVs was noticeably higher under the two most acidic conditions (>100 under HPr81 and HCl) than under all other conditions (<30). Furthermore, HPr81 and HCl reactors shared a substantial number of differentially abundant ASVs (64 negatively affected and 10 positively affected), which

represents the largest groups in the upset plot analysis (Figure 4). This suggests largely common adaptive responses of the microbial communities facing a low pH (see also Figures S93 and S94). Across the dataset of the second tests, the number of differentially abundant ASVs was negatively correlated with the methane production rates estimated using the Gompertz model ($R^2 = 0.9698$, Figure S96). This supports the strong link between the level of AD impairment and the extent of microbial community reshaping.

3.6 Adaptation of microbial community to propionate (Pr-) without acidity shift

Given the predominant impact of acidity on microbial communities, NaPr exposures were the most suitable conditions for evaluating the specific effect of propionate on microbial community composition, as the reactor pH was much less affected than under HPr exposures.

NaPr81 was analyzed first since it had the strongest effect on microbial communities (Figure 5A) and inhibited only moderately methane production (Figure 1B and 1C). We identified 12 ASVs as highly robust regarding adaptation to Pr^-, as they were differentially abundant when comparing NaPr81 to Ctrl and NaPr81 to NaCl81, but not when comparing NaCl81 to Ctrl (Tables S6). Among them, we focused on the most abundant ones (reaching approximately 1% in at least one sample) and those showing strong reproducibility.

In details, the abundances of ASV_2 (order Bacteroidales, family Prolixibacteraceae) and ASV_208 (order Syntrophorhabdales, genus *Syntrophorhabdus*) were reduced under NaPr81, whereas ASV_68 (order Xanthomonadales, genus *Thermomonas*) and ASV_703 (order Synergistales, family Synergistaceae) were on the contrary favoured under the same condition. Members of Prolixibateraceae are rod-shaped, non-motile, facultative anaerobes, frequently isolated from coastal sediments or waters, capable of fermenting certain carbohydrates (Huang et al., 2014; Zhou et al., 2019). The sole isolated bacterium belonging to *Syntrophorhabdus* can oxidize aromatic compounds in syntrophy with hydrogenotrophic methanogens (Qiu et al., 2008). As mentioned above, some *Thermomonas* strains can assimilate propionate (Denner et al., 2015),

which may have explained their higher abundance under the high NaPr concentration. According to the MIDAS database (Dueholm et al., 2024), Synergistaceae bacteria ferment certain acids and amino acids but not systematically carbohydrates, producing H_2 and other metabolites, sometimes propionate.

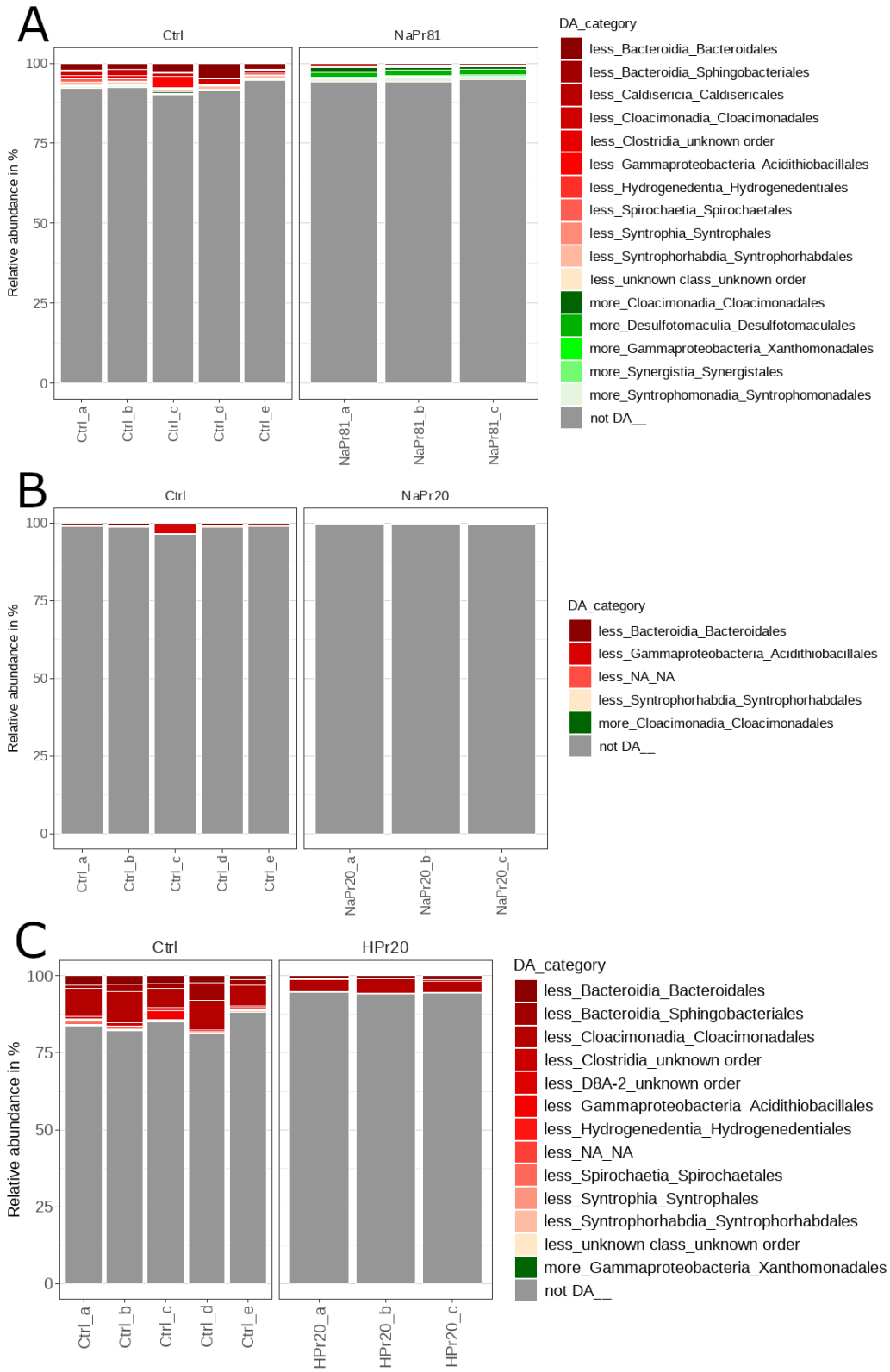

Figure 5. Taxonomy and relative abundance of differentially abundant ASVs identified under various conditions, compared to Ctrl. The results are based on the number of 16S rDNA amplicon reads and are shown at the taxonomic level of the order. Red indicates the ASVs that were significantly less abundant in the treatment compared to Ctrl. Green indicates the ASVs that were significantly more abundant in the treatment compared to Ctrl. (A) Comparison of NaPr81 to Ctrl (B) Comparison of NaPr20 to Ctrl (C) Comparison of HPr20 to Ctrl.

As expected, NaPr20 had a much more limited effect on both methane production and microbial community composition compared to NaPr81. ASV_109 (Bacteroidales, Rikenellaceae, S50 wastewater-sludge group) and ASV_453 (Syntrophorhabdales, *Syntrophorhabdus*) remain noteworthy, however, as they were significantly inhibited under NaPr20, possibly corresponding to strains highly sensitive to propionate. Nevertheless, these ASVs exhibited limited abundances based on the 16S metabarcoding data (<1% in the control reactors). Rikenellaceae includes obligate anaerobic fermenters according to MIDAS database (Dueholm et al., 2024).

3.7 Adaptation of microbial community to propionate (Pr-) with acidity shift

HPr20 was subsequently compared to Ctrl in the second tests, to further identify biomarker candidates for early warning during HPr inhibition. Three ASVs were particularly notable (Figure 5C, Table S6) since they both exhibited significant abundances (≥ 1% in at least one treatment) and had lower abundances relative to Ctrl. ASV_6 (order Cloacimonadales, genus W5), ASV_16 (order Bacteroidales, family Rikenellaceae, genus DMER64), and ASV_21 (order Sphingobacteriales, family ST12-K33). Although less pronounced, it is also worth noting the presence of ASV_68 (order Xanthomonadales, genus *Thermomonas*) in two out of three HPr20 reactors, while it was not detected in any of the Ctrl reactors.

Finally, to identify the most robust biomarker candidates for inhibition caused by HPr, we compared the candidates obtained in the first and second tests. Two families,

Hungateiclostridiaceae and ST-12K33 (Sphingobacteriales), were negatively affected during both test series. The pattern was notably clear for ST-12K33 (Sphingobacteriales, Figure 2C-D), which is therefore a promising candidate. However, little is known about its metabolism during AD: further investigation is needed to understand its function and its relevance as a potential biomarker.

4. Discussion

The first and second tests were conducted under very similar conditions, as both the raw and digested sludge originated from the same plant and digester. Moreover, all incubations were in AMPTS II, under mesophilic, batch conditions. A certain repeatability was thus expected. Despite this, the effects detected on microbial community composition showed some differences, highlighting the challenge of identifying generic biomarkers. Notably, the family Oscillospiraceae, which was selected under HPr13 and HPr20 during the first tests (Figure 3E), displayed a significantly distinct pattern in the second tests, being detected only in the most acidic conditions, specifically under HPr81 and HCl. It should be noted, however, that no longitudinal monitoring was performed during the second tests, which could partly explain this apparent difference, as Oscillospiraceae abundance seemed to decrease at later time points in the first tests. This generally underlines the need for a comprehensive characterization of microbial dynamics and highlights the importance of further validating candidate biomarkers under conditions close to the industrial scale. It is worth noting that in one of our previous studies (Camargo et al.), acid inhibition with HPr accumulation naturally occurred during the dry co-digestion of wastewater treatment sludge and horse manure, due to high organic loading; some of the microorganisms negatively affected under these conditions were similar to those identified in the present study, in at least one test series. These included members of the families Sedimentibacteraceae, Smithellaceae, and ST-12K33 (Sphingobacteriales), which were also inhibited by HPr in the present study. *Sedimentibacter* was also negatively affected during the semi-continuous mesophilic digestion of dairy manure disrupted through HPr spikes (Khafipour et al., 2020). The same study documented

a decrease in the abundance of *Syntrophomonas* in response to HPr, which is also consistent with our observations. During our study, we observed a strong negative effect of HPr on the relative abundance of archaea. Determining the methanogenesis pathways was, however, challenging in the absence of functional analysis, especially since one of the most dominant methanogens in our study had a multi-hit affiliation, pointing to several possible distinct metabolisms. Our findings are nevertheless consistent with the idea that methanogens are highly sensitive to perturbations, which often affect their composition and abundance (Han et al., 2020; Khafipour et al., 2020; Li et al., 2017).

When propionic acid was added to the reactors, one might have expected antagonistic effects on propionate-consuming bacteria: on the one hand, selection of these bacteria due to an increase in available substrate; on the other hand, a negative effect due to acidic inhibition. In our dataset, a significant number of families possibly contained SPOB, including Acidaminococcaceae, Cloacimonadaceae, Christensenellaceae, Comamonadaceae, Peptococcaceae, Smithellaceae, Syntrophobacteraceae, Syntrophomonadaceae and families from the order Desulfotomaculales (Westerholm et al., 2022). However, this activity was difficult to confirm on the basis of 16S rDNA sequencing alone. Indeed, our method yielded taxonomic assignation at the genus level, and it is known that not all species within a given genus are SPOB. For instance, *Smithella propionica* is currently the only known SPOB within the *Smithella* genus (Westerholm et al., 2022). Nevertheless, certain ASVs had abundance profiles compatible with a SPOB activity, showing an increase in relative abundance at moderate propionic acid concentrations, and a decrease at high propionic acid concentrations. This was the case for ASV_46 during the first tests (Syntrophomonadaceae, *Syntrophomonas*), which had the highest abundance under Ctrl on day 2, under HPr13 on day 4, and very low abundances under HPr20 and HPr81.

A previous study evidenced that anaerobic digesters can tolerate propionate concentrations as high as 50 mM of NaPr (4,800 $mg.L^{-1}$) (Ahring et al., 1995). More recently, it was shown that 41.6 mM of NaPr (4,000 $mg.L^{-1}$) can be fully degraded in batch reactors (Yang et al., 2015). The present

study further confirms the moderate resilience of AD reactors to NaPr molar concentrations up to 81 mM (7,750 mg.L^{-1}), which is far higher than the threshold reported for its acid form (12 mM of HPr, equivalent to 900 mg.L^{-1}) (Wang et al., 2009; Han et al., 2020).

The maximum VFA concentration at which AD can operate depends on numerous factors. On one hand, the propionate concentration is always reported relative to the media volume. It does not accurately describe how propionate locally surrounds and interacts with microbial cells. The ratios between inoculum, raw sludge and propionate concentrations in reactors could play a key role and partially explain the differences observed among various studies (e.g. 6,4 g VS.L^{-1} / 54 mM in Han et al. (2020) versus 22,4 g VS.L^{-1} / 81 mM in our study). On the other hand, the tolerance of AD reactors to propionic acid and its conjugated base differs greatly. Propionic acid is one of the intermediate metabolites produced during acidogenesis. However, it is rapidly dissociated into propionate ions upon exposure to AD media, which are usually basic. Neither the addition of external propionic acid nor propionate salts can perfectly simulate the *in-situ* production and inhibition of propionic acid within microbial cells. The present study distinguishes the effect of pH drop and that of propionate as a substrate on the inhibition methanogenesis.

4. Conclusions

In this study, we observed a negative effect of propionic acid on methane production rate during the AD of wastewater treatment sludge, and this negative effect increased with propionic acid concentration. A partial decrease in the methane production rate was detected when adding 13 mM of propionic acid (1,000 mg.L^{-1}), while total inhibition occurred for 81 mM (6,000 mg.L^{-1}). Through comparison with the effects of adding sodium propionate, sodium chloride, or of decreasing the pH, it appeared that this inhibition was largely attributed to the H^+ counter-ion, as it caused a decrease in pH. The composition of the microbial communities was significantly modified in the presence of propionate, with this adaptation specifically depending on the nature and concentration of the compound added. A variety of functional groups were affected, including

syntrophs and methanogenic archaea. For the latter, the relative abundance decreased significantly in the presence of propionic acid, consistent with the negative effects observed on methane production rate, and with previous studies. Several microbial groups highly sensitive to propionic acid were identified in our tests, in particular the family ST-12K33 (order Sphingobacteriales). Further investigation of its function could improve our understanding of their importance as a functional group or candidate biomarker. To advance the development of operational biomarkers, further attention should be given to gaining a deeper understanding of how propionate-related inhibition occurs under actual operational conditions, typically under continuous feeding.

Acknowledgements

This study was funded by the French research program MOCOPEE.

Author Contributions

XL: Conceptualization, Formal analysis, Writing – original draft, **CS**: Investigation, Formal analysis, **VJ**: Data curation, Formal analysis, Writing – review and editing, **AP**: Conceptualization, Supervision, Writing – review and editing, **LA**: Investigation, Conceptualization, Supervision, Writing – review and editing, **TR**: Conceptualization, Supervision, Writing – review and editing, **S G-R**: Conceptualization, **VR**: Conceptualization, **CL**: Investigation, Conceptualization, **CB**: Investigation, Writing – review and editing, **CM**: Software, Writing – review and editing, **OC**: Conceptualization, Writing – review and editing, **AB**: Conceptualization, Formal analysis, Writing – original draft, **C R-A**: Conceptualization, Supervision, Writing – review and editing.

References

Ahring, B.K., Sandberg, M., Angelidaki, I. 1995. Volatile fatty acids as indicators of process imbalance in anaerobic digestors. *Applied Microbiology and Biotechnology*, **43**(3), 559-565.

Alavi-Borazjani, S.A., Capela, I., Tarelho, L.A.C. 2020. Over-acidification control strategies for enhanced biogas production from anaerobic digestion: A review. *Biomass and Bioenergy*, **143**, 105833.

Bernard, M., Rué, O., Mariadassou, M., Pascal, G. 2021. FROGS: a powerful tool to analyse the diversity of fungi with special management of internal transcribed spacers. *Briefings in Bioinformatics*, **22**(6), bbab318.

Callahan, B.J., McMurdie, P.J., Rosen, M.J., Han, A.W., Johnson, A.J.A., Holmes, S.P. 2016. DADA2: High-resolution sample inference from Illumina amplicon data. *Nature Methods*, **13**(7), 581-583.

Calusinska, M., Goux, X., Fossépré, M., Muller, E.E.L., Wilmes, P., Delfosse, P. 2018. A year of monitoring 20 mesophilic full-scale bioreactors reveals the existence of stable but different core microbiomes in bio-waste and wastewater anaerobic digestion systems. *Biotechnology for Biofuels*, **11**(1), 196.

Camargo, F., Roose-Amsaleg, C., Guérin, S., Lacroix, C., Goubet, A., Bureau, C., Madigou, C., Midoux, C., Leonel, L.P., Tonetti, A.L. Acidic Inhibition and Microbial Community Adaptation During Mesophilic Dry Anaerobic Co-Digestion of Racehorse Manure and Organic Household Waste. *Available at SSRN 4631686*.

Campanaro, S., Treu, L., Kougias, P.G., De Francisci, D., Valle, G., Angelidaki, I. 2016. Metagenomic analysis and functional characterization of the biogas microbiome using high throughput shotgun sequencing and a novel binning strategy. *Biotechnology for Biofuels*, **9**(1), 26.

Chen, Y., Cheng, J.J., Creamer, K.S. 2008. Inhibition of anaerobic digestion process: A review. *Bioresource Technology*, **99**(10), 4044-4064.

Clark, R.H., Speece, R.E. 1971. The pH tolerance of anaerobic digestion. *Advances in Water Pollution Research*, **1**, 1-13.

Demirel, B., Yenigün, O. 2002. The Effects of Change in Volatile Fatty Acid (VFA) Composition on Methanogenic Upflow Filter Reactor (UFAF) Performance. *Environmental Technology*, **23**(10), 1179-1187.

Denner, E.B.M., Kämpfer, P., Busse, H.-J. 2015. Thermomonas. in: *Bergey's Manual of Systematics of Archaea and Bacteria*, pp. 1-6.

Dueholm, M.K.D., Andersen, K.S., Korntved, A.-K.C., Rudkjøbing, V., Alves, M., Bajón-Fernández, Y., Batstone, D., Butler, C., Cruz, M.C., Davidsson, Å., Erijman, L., Holliger, C., Koch, K., Kreuzinger, N., Lee, C., Lyberatos, G., Mutnuri, S., O'Flaherty, V., Oleskowicz-Popiel, P., Pokorna, D., Rajal, V., Recktenwald, M., Rodríguez, J., Saikaly, P.E., Tooker, N., Vierheilig, J., De Vrieze, J., Wurzbacher, C., Nielsen, P.H. 2024. MiDAS 5: Global diversity of bacteria and archaea in anaerobic digesters. *Nature Communications*, **15**(1), 5361.

EUROSTAT. Sewage Sludge Production and Disposal Available online: http://appsso.eurostat.ec.europa.eu/nui/show.do?lang=en&dataset=env_ww_spd.

Gophna, U., Konikoff, T., Nielsen, H.B. 2017. Oscillospira and related bacteria – From metagenomic species to metabolic features. *Environmental Microbiology*, **19**(3), 835-841.

Han, Y., Green, H., Tao, W. 2020. Reversibility of propionic acid inhibition to anaerobic digestion: Inhibition kinetics and microbial mechanism. *Chemosphere*, **255**, 126840.

Holliger, C., Alves, M., Andrade, D., Angelidaki, I., Astals, S., Baier, U., Bougrier, C., Buffière, P., Carballa, M., de Wilde, V., Ebertseder, F., Fernández, B., Ficara, E., Fotidis, I., Frigon, J.-C., de Laclos, H.F., Ghasimi, D.S.M., Hack, G., Hartel, M., Heerenklage, J., Horvath, I.S., Jenicek, P., Koch, K., Krautwald, J., Lizasoain, J., Liu, J., Mosberger, L., Nistor, M., Oechsner, H., Oliveira, J.V., Paterson, M., Pauss, A., Pommier, S., Porqueddu, I., Raposo, F., Ribeiro, T., Rüsch Pfund, F., Strömberg, S., Torrijos, M., van Eekert, M., van Lier, J., Wedwitschka, H., Wierinck, I. 2016. Towards a standardization of biomethane potential tests. *Water Science and Technology*, **74**(11), 2515-2522.

Huang, X.-F., Liu, Y.J., Dong, J.-D., Qu, L.-Y., Zhang, Y.-Y., Wang, F.-Z., Tian, X.-P., Zhang, S. 2014. Mangrovibacterium diazotrophicum gen. nov., sp. nov., a nitrogen-fixing bacterium isolated from a mangrove sediment, and proposal of Prolixibacteraceae fam. nov. *International Journal of Systematic and Evolutionary Microbiology*, **64**(Pt_3), 875-881.

Imachi, H., Sakai, S., Kubota, T., Miyazaki, M., Saito, Y., Takai, K. 2016. Sedimentibacter acidaminivorans sp. nov., an anaerobic, amino-acid-utilizing bacterium isolated from marine subsurface sediment. *International Journal of Systematic and Evolutionary Microbiology*, **66**(3), 1293-1300.

Jiang, C., Peces, M., Andersen, M.H., Kucheryavskiy, S., Nierychlo, M., Yashiro, E., Andersen, K.S., Kirkegaard, R.H., Hao, L., Høgh, J., Hansen, A.A., Dueholm, M.S., Nielsen, P.H. 2021. Characterizing the growing microorganisms at species level in 46 anaerobic digesters at Danish wastewater treatment plants: A six-year survey on microbial community structure and key drivers. *Water Research*, **193**, 116871.

Jiang, Y., Dennehy, C., Lawlor, P.G., Hu, Z., McCabe, M., Cormican, P., Zhan, X., Gardiner, G.E. 2018. Inhibition of volatile fatty acids on methane production kinetics during dry co-digestion of food waste and pig manure. *Waste Management*, **79**, 302-311.

Jouan-Rimbaud Bouveresse, D., Rutledge, D.N. 2024. A synthetic review of some recent extensions of ComDim. *Journal of Chemometrics*, **38**(5), e3454.

Khafipour, A., Jordaan, E.M., Flores-Orozco, D., Khafipour, E., Levin, D.B., Sparling, R., Cicek, N. 2020. Response of Microbial Community to Induced Failure of Anaerobic Digesters Through Overloading With Propionic Acid Followed by Process Recovery. *Frontiers in Bioengineering and Biotechnology*, **8**.

Kirkegaard, R.H., McIlroy, S.J., Kristensen, J.M., Nierychlo, M., Karst, S.M., Dueholm, M.S., Albertsen, M., Nielsen, P.H. 2017. The impact of immigration on microbial community composition in full-scale anaerobic digesters. *Scientific Reports*, **7**(1), 9343.

Krohn, C., Khudur, L., Dias, D.A., van den Akker, B., Rees, C.A., Crosbie, N.D., Surapaneni, A., O'Carroll, D.M., Stuetz, R.M., Batstone, D.J., Ball, A.S. 2022. The role of microbial ecology in improving the performance of anaerobic digestion of sewage sludge. *Frontiers in Microbiology*, **13**.

Li, Y., Zhang, Y., Sun, Y., Wu, S., Kong, X., Yuan, Z., Dong, R. 2017. The performance efficiency of bioaugmentation to prevent anaerobic digestion failure from ammonia and propionate inhibition. *Bioresource Technology*, **231**, 94-100.

Liu, Y., Whitman, W.B. 2008. Metabolic, Phylogenetic, and Ecological Diversity of the Methanogenic Archaea. *Annals of the New York Academy of Sciences*, **1125**(1), 171-189.

Love, M.I., Huber, W., Anders, S. 2014. Moderated estimation of fold change and dispersion for RNA-seq data with DESeq2. *Genome Biology*, **15**(12), 550.

McMurdie, P.J., Holmes, S. 2013. phyloseq: An R Package for Reproducible Interactive Analysis and Graphics of Microbiome Census Data. *PLOS ONE*, **8**(4), e61217.

Poirier, S., Bize, A., Bureau, C., Bouchez, T., Chapleur, O. 2016. Community shifts within anaerobic digestion microbiota facing phenol inhibition: Towards early warning microbial indicators? *Water Research*, **100**, 296-305.

Puig-Castellví, F., Cardona, L., Jouan-Rimbaud Bouveresse, D., Cordella, C.B.Y., Mazéas, L., Rutledge, D.N., Chapleur, O. 2020. Assessment of the microbial interplay during anaerobic co-digestion of wastewater sludge using common components analysis. *PLOS ONE*, **15**(5), e0232324.

Pullammanappallil, P.C., Chynoweth, D.P., Lyberatos, G., Svoronos, S.A. 2001. Stable performance of anaerobic digestion in the presence of a high concentration of propionic acid. *Bioresource Technology*, **78**(2), 165-169.

Qiao, W., Takayanagi, K., Niu, Q., Shofie, M., Li, Y.Y. 2013. Long-term stability of thermophilic co-digestion submerged anaerobic membrane reactor encountering high organic loading

rate, persistent propionate and detectable hydrogen in biogas. *Bioresource Technology*, **149**, 92-102.

Qiu, Y.-L., Hanada, S., Ohashi, A., Harada, H., Kamagata, Y., Sekiguchi, Y. 2008. Syntrophorhabdus aromaticivorans gen. nov., sp. nov., the First Cultured Anaerobe Capable of Degrading Phenol to Acetate in Obligate Syntrophic Associations with a Hydrogenotrophic Methanogen. *Applied and Environmental Microbiology*, **74**(7), 2051-2058.

Roe Andrew, J., McLaggan, D., Davidson, I., O'Byrne, C., Booth Ian, R. 1998. Perturbation of Anion Balance during Inhibition of Growth of Escherichia coli by Weak Acids. *Journal of Bacteriology*, **180**(4), 767-772.

Rohart, F., Gautier, B., Singh, A., Lê Cao, K.-A. 2017. mixOmics: An R package for 'omics feature selection and multiple data integration. *PLOS Computational Biology*, **13**(11), e1005752.

Sakai, S., Ehara, M., Tseng, I.-C., Yamaguchi, T., Bräuer, S.L., Cadillo-Quiroz, H., Zinder, S.H., Imachi, H. 2012. Methanolinea mesophila sp. nov., a hydrogenotrophic methanogen isolated from rice field soil, and proposal of the archaeal family Methanoregulaceae fam. nov. within the order Methanomicrobiales. *International Journal of Systematic and Evolutionary Microbiology*, **62**(Pt_6), 1389-1395.

Sawyer, C.N., Howard, F.S., Pershe, E.R. 1954. Scientific Basis for Liming of Digesters. *Sewage and Industrial Wastes*, **26**(8), 935-944.

Scarlat, N., Dallemand, J.-F., Fahl, F. 2018. Biogas: Developments and perspectives in Europe. *Renewable Energy*, **129**, 457-472.

Sekiguchi, Y. 2015. Syntrophomonas. in: *Bergey's Manual of Systematics of Archaea and Bacteria*, pp. 1-11.

Shrestha, B., Hernandez, R., Fortela, D.L.B., Sharp, W., Chistoserdov, A., Gang, D., Revellame, E., Holmes, W., Zappi, M.E. 2020. A Review of Pretreatment Methods to Enhance Solids Reduction during Anaerobic Digestion of Municipal Wastewater Sludges and the Resulting

Digester Performance: Implications to Future Urban Biorefineries. in: *Applied Sciences*, Vol. 10.

Sikora, A., Detman, A., Chojnacka, A., Błaszczyk, M.K. 2017. Anaerobic digestion: I. A common process ensuring energy flow and the circulation of matter in ecosystems. II. A tool for the production of gaseous biofuels. *Fermentation processes*, **14**, 271.

Sousa, D.Z., Smidt, H., Alves, M.M., Stams, A.J.M. 2007. Syntrophomonas zehnderi sp. nov., an anaerobe that degrades long-chain fatty acids in co-culture with Methanobacterium formicicum. *International Journal of Systematic and Evolutionary Microbiology*, **57**(3), 609-615.

Team, R.C. 2021. A language and environment for statistical computing. *(No Title)*.

Theuerl, S., Klang, J., Heiermann, M., De Vrieze, J. 2018. Marker microbiome clusters are determined by operational parameters and specific key taxa combinations in anaerobic digestion. *Bioresource Technology*, **263**, 128-135.

Verstraete, W., Mertens, B. 2004. Chapter 5 The key role of soil microbes. in: *Developments in Soil Science*, (Eds.) P. Doelman, H.J.P. Eijsackers, Vol. 29, Elsevier, pp. 127-157.

Wang, Y., Zhang, Y., Wang, J., Meng, L. 2009. Effects of volatile fatty acid concentrations on methane yield and methanogenic bacteria. *Biomass and Bioenergy*, **33**(5), 848-853.

Westerholm, M., Calusinska, M., Dolfing, J. 2022. Syntrophic propionate-oxidizing bacteria in methanogenic systems. *FEMS Microbiology Reviews*, **46**(2), fuab057.

Yang, Y., Chen, Q., Guo, J., Hu, Z. 2015. Kinetics and methane gas yields of selected C1 to C5 organic acids in anaerobic digestion. *Water Research*, **87**, 112-118.

Zhou, L.-Y., Yu, Z.-L., Xu, W., Mu, D.-S., Du, Z.-J. 2019. Maribellus luteus gen. nov., sp. nov., a marine bacterium in the family Prolixibacteraceae isolated from coastal seawater. *International Journal of Systematic and Evolutionary Microbiology*, **69**(8), 2388-2394.